Thermo-Economic Analysis of a Geothermal-Based High Temperature Heat Pump

Pietro Ungar[1,*], Daniele Fiaschi[1], Giampaolo Manfrida[1]

[1]University of Florence, Department of Industrial Engineering, Florence, Italy

*Corresponding Author: pietro.ungar@unifi.it

ABSTRACT

In light of growing environmental concerns, there's a heightened drive to lessen the industrial sector's reliance on natural gas. A system capable of providing mid-low temperature heat (ranging from 90°C to 120°C) in a sustainable and cost-effective way is increasingly attractive to the industrial sector. In this study, a detailed exergo-economic analysis of possible geothermal-based system has been performed to asses the economic feasibility of the proposed solution. Moreover, the performance of the sCO2-based system will be compared with a water loop for geothermal heat extraction coupled with an High-Temperature Heat Pump to asses the behaviour of the proposed scheme under different reservoir condition. In the scope of this study, it has been also considered the possibility of power cogeneration which could be achieved, for the sCO2-based system, exploiting the natural pressurisation of the fluid due to the thermosyphon effect, and that will be even more appealing for the industrial sector. The performed calculation have shown that the LCOH of the system is expected to be in line with other comparable technologies with the sCO2-based system being more promising for the production of lower temperature heat and for geological setting with lower geothermal gradient.

1 Introduction

Efficient production and distribution of renewable energy are key challenges to reaching the net-zero target by 2050. In 2021, heat production accounted for half of the total energy consumption in the world (IEA (2022)), with 51% of this demand coming from industrial processes, which commonly require heat temperatures above 80°C (IEA-IETS (2014)). Additionally, a study published in 2019 by the Oxford Institute for Energy Studies found that industrial processes needing heat in the temperature range of 100°C – 500°C represent 30% of the total industrial heat requirements, mainly in the paper and print, food, and chemical sectors (Honore (2019)). High Temperature Heat Pumps (HTHP) are one of the most promising technologies for the decarbonization of industrial heat demand. Consequently, there has been growing scientific interest in this field in recent years.

1.1 High-Temperature Heat Pumps

Arpagaus et al. (2018) conducted a comprehensive review of the current market and state of the art for high-temperature heat pumps, emphasizing the need for progressive development of HTHPs capable of delivering temperatures over 140°C.A detailed analysis of possible configurations for these applications was published by Zühlsdorf et al. (2019). Their paper focuses on the production of steam for industrial applications, examining two different HTHP configurations that have proven competitive, in terms of levelized cost of heat, with other technologies. According to the authors of this study, the most promising cycles for industrial steam production are a steam compression system and a sCO2 reversed Bryton cycle. These cycles, slightly modified for integration with the geothermal system, have been analyzed in this

https://doi.org/10.52202/077185-0109

study. As pointed out by Arpagaus (Arpagaus et al. (2018)), the efficiency of an HTHP system is directly related to the source temperature; hence, coupling the heat pump with a geothermal system could be extremely beneficial in terms of energy consumption.

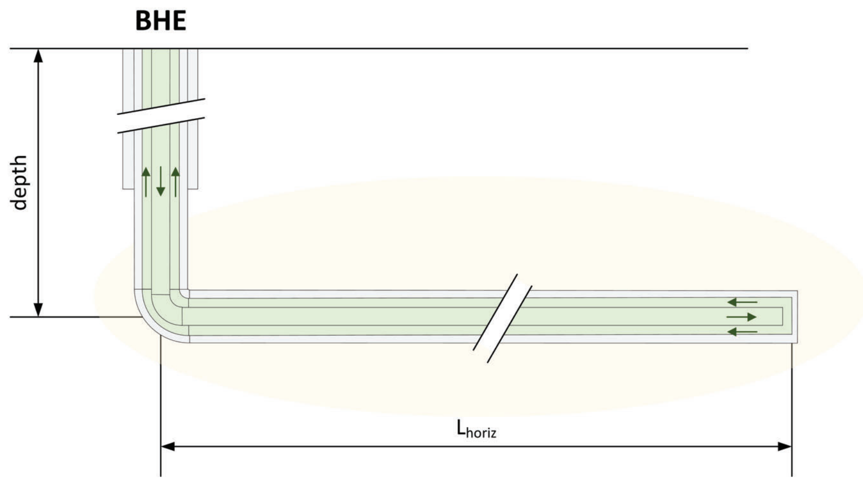

Figure 1: Schemes of a concentric BHE well

1.2 Well Model

Multiple models for geothermal wells have been considered throughout the years. In this work, we have focused on analyzing the behavior of a closed-loop borehole heat exchanger (BHE). The considered well, sketched in Figure 1, consists of two concentric pipes through which the fluid circulates and is heated by exchanging heat with the surrounding rocks. This type of well has been extensively studied in recent years by multiple researchers in both its vertical (Sun et al. (2018a) and Galoppi et al. (2015)) and horizontal (Sun et al. (2018b)) configuration. Recently, a European project has been awarded to enhance the development of these wells (European Project (2022)).

1.3 Analysed Configurations

Two different surface installation schemes have been considered for this analysis (as shown in Figure 2). The water-based scheme is simpler and has been used primarily for benchmarking the CO_2-based results. In this configuration, the water, heated in the well, powers an HTHP's evaporator before being directly re-injected into the well to be heated again.

The CO_2-based scheme, on the other hand, is slightly more complex: the CO_2 is injected into the well as saturated liquid evaporating in the horizontal section, resulting in the development of an important thermosyphon effect. The heated and compressed CO_2 is then mixed with the eventual CO_2 that accumulates in the separator and is further compressed to reach the desired temperature level (T_{max}). The CO_2 is then cooled down in the main heat exchanger (providing power to the heat pump users) and then expanded to recover part of the compressor power. Before the expansion there's the possibility of further cooling the CO_2 to decrease the quality of the CO_2 coming out from the turbine.

2 Methodology

2.1 Thermodynamic Model

To evaluate the behaviour of these systems two different sub-models have been developed: the model of the well and the model of the surface installation.

https://doi.org/10.52202/077185-0109

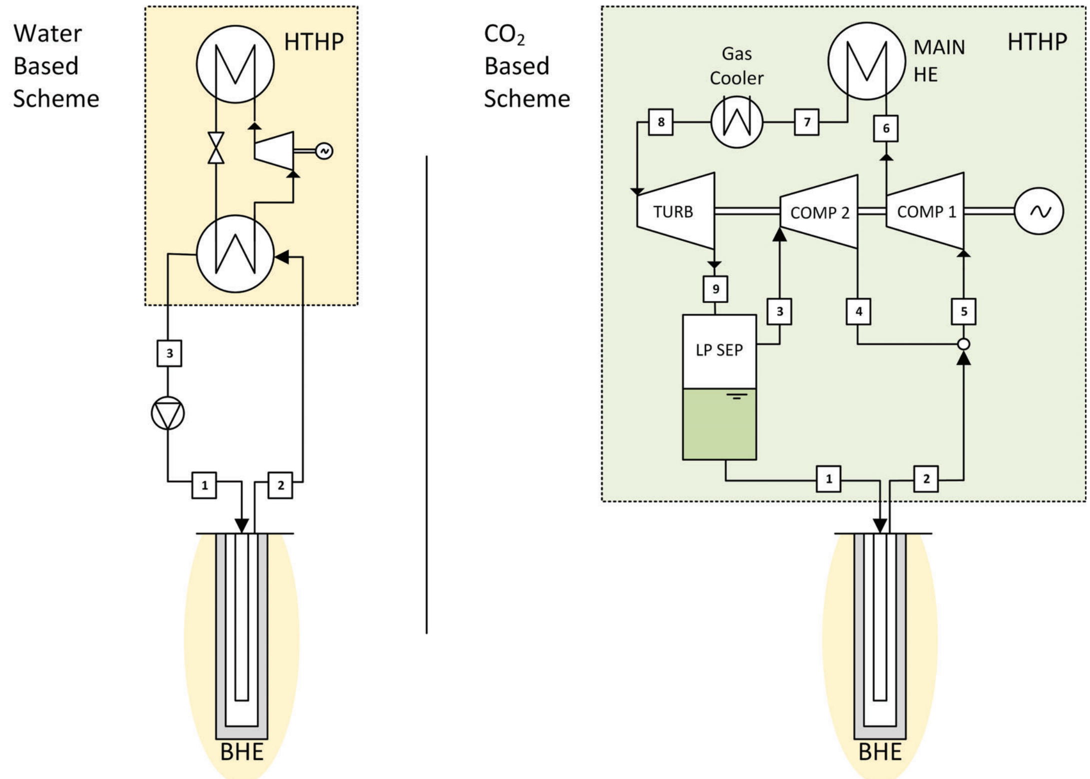

Figure 2: Schemes considered for the analysis. Left: Water-based system coupled with an high temperature heat pump, Right: CO_2-based system

2.1.1 Well Model The model developed by Ungar in his PhD thesis (Ungar (2023)) has been used to predict the behaviour of the fluid inside the well. The model works by integrating the momentum (eq.1) and energy (eq.2) balance equation tough-out the well.

$$\frac{dp}{dl} = -\left(\rho g cos\theta \ + dp_{loss}\right) \tag{1}$$

$$\frac{dh}{dl} = -\left(g cos\theta \ - d\dot{q}_{tot}/\dot{m}_{well}\right) \tag{2}$$

where θ is the inclination of the well with respect to the vertical direction, $\dot{m}_{well}$ is the flow rate of teh fluid inside the well, $d\dot{q}_{tot}$ and dp_{loss} are the derivative heat exchanged and pressure losses of the fluid.

The system composed of (1) and of (2) is integrated in python using a explicit 5th order Runge-Kutta method (Dormand and Prince (1980)) as implemented in the SciPy python package (Virtanen et al. (2020)).

The pressure losses are evaluated using the Churchill correlation (Churchill (1977)) for the estimation of friction factor f:

$$dp_{loss} = f\frac{1}{2\rho d_{well}}\left(\frac{\dot{m}_{well}}{A_{flow}}\right)^2 \tag{3}$$

To account for heat transfer in rocks formation around the well without having to solve a finite difference model of the temperature distribution in the surrounding, a semi-analytical correlation has been implemented (Zhang et al. (2011)):

$$R_{rocks} = \frac{d_{well}}{2k_{rocks}g(t_d)} \tag{4}$$

https://doi.org/10.52202/077185-0109

with:

$$g(t_d) = \begin{cases} \frac{1}{2} + (\pi t_d)^{-\frac{1}{2}} - \frac{1}{4}\left(\frac{t_d}{\pi}\right)^{\frac{1}{2}} + \frac{1}{8}t_d, & \text{if } t_d < 2.8 \\ \frac{2}{ln(4t_d)-2\gamma} - \frac{2\gamma}{(ln(4t_d)-2\gamma)^2}, & \text{if } t_d \geq 2.8 \end{cases} \tag{5}$$

Where, in (5):

- $t_d = 4\alpha_{rocks} t/d_{well}^2$ is a dimensionless time (t in seconds)
- $\alpha_{rocks} = k_{rocks}/\rho_{rocks} C_{p_{rocks}}$ is the thermal diffusivity of the rocks
- γ is Euler's constant
- d_{well} is the external diameter of the well

To keep the water-based and the CO_2-based solutions comparable, the same well has been considered for both. The main design parameter are listed in the table below:

Table 1: Geothermal BHE design parameters

Symbol	Description	Value
Δz_{well}	Depth of the horizontal section	3km
L_{well}	Overall length of the well	6.5km
$d_{cas_{id}}$	External diameter of the annulus	16cm
$d_{tub_{od}}$	Internal diameter of the annulus	13cm
$d_{tub_{id}}$	Internal diameter of the tubing	10cm

The geothermal gradient of the rocks around the well (∇T_{geo}) has been varied to test different geological conditions. The flow rate that circulates inside the well ($\dot{m}_{well}$) has been varied as well.

2.1.2 CO_2-Based Heat Pump Model The CO_2-based heat pump model has been developed in EES (Klein (2020)). The pressure at the outlet of the main compressor *(*COMP 1 *in Figure 2)* is adjusted according to the inlet condition to reach the desired temperature in point 6 *(T_{max})*. The temperature at the inlet of the turbine *($T_{turb_{in}}$)* is an important parameter as well and can be optimised. In fact, lowering $T_{turb_{in}}$ result in a decreased turbine power output but it will also decrease the amount of vapour that has to be re-compressed trough the compressor *COMP 2*.

Some fixed parameters were assumed in the model. They are listed in the table below:

Table 2: CO_2-based HTHP - Fixed Parameters

Symbol	Description	Value
η_{comp}	Compressor Efficiency	0.8
η_{turb}	Turbine Efficiency	0.75
ΔT_{HE}	Temperature range inside the main heat exchanger	40°C
T_{sat}	Saturation Temperature in the low pressure separator *(LP SEP)*	10°C

2.1.3 Water-Based Heat Pump Model Following the approach described in (Ungar et al. (2023)), the heat pump connected to the water-based well has been modelled considering a fixed exergy efficiency of 0.4, which has been chosen based on some experimental results from literature (Bilgen and Takahashi (2002)). Knowing the exergy efficiency is possible to estimate the electrical power demand as:

$$\dot{W}_{HP} = \frac{1}{\eta_{exergy}}\left(1 - \frac{T_{low}}{T_{high}}\right)\dot{Q}_{HP} = \frac{1}{0.4}\left(1 - \frac{T_{low}}{T_{high}}\right)\dot{Q}_{HP} \tag{6}$$

https://doi.org/10.52202/077185-0109

Where T_{low} has been supposed to be equal to the temperature of point 3 (the index refers to Fig 2) and hence depends on the water temperature range in the HE which can be optimised (a lower temperature in 3 means an higher heat extraction rate from the well but also requires some additional work from the heat pump which has to overcome an higher temperature difference).

Once both models have been solved an exergy analysis have been conducted using an in-house developed tool called *"3ETool"* (Fiaschi et al. (2022)).

2.1.4 Economic Analysis The Levelized Cost of Heat (LCOH) has been evaluated for both the solutions following the same approach described in a previous paper (Ungar et al., 2023):

$$LCOH = \frac{C_{tot}\beta + \dot{W}_{tot}c_{el}}{\dot{Q}_{DH}}, \quad \beta = \frac{1 + \alpha OM_{ratio}}{\alpha h_y}, \quad \alpha = \frac{1 - (1+i)^{-L_e}}{i} \tag{7}$$

With $\dot{W}_{tot}$ being the net electrical power required to run the system (or sold to the grid if the conditions allow for co-generation) and $\dot{Q}_{DH}$ the power delivered to the heat user. In addition, C_{tot} is the overall investment cost to setup the system, c_{el} the cost of electricity. β is a multiplier that encompasses the effects of operation an maintenance cost ($C_{om} = OM_{ratio}C_{tot}$, with $OM_{ratio} = 5\%/year$) and the discounting of cash flows. Finally, $L_e = 20years$ is the expected lifetime of the plant, $i = 4\%/year$ is the interest rate and $h_y = 8000hours/year$ is the expected operational time of the system, that are reasonable values if an industrial application is considered.

C_{tot} is evaluated differently for the water-based and the CO_2-based systems:

$$C_{tot_{H_2O}} = C_{well} + C_{HP} \tag{8}$$

$$C_{tot_{CO_2}} = C_{well} + C_{turb} + \sum C_{comp} + \sum C_{HE} \tag{9}$$

The different correlations that have been used to estimate the cost of the system components are listed in Table 3 (in the appendix).

3 Results

3.1 Well Behaviour

The well behaves very differently between the water-based and CO_2-based scenario. As shown in Figure 3, in the water-based case, the pressure decrease inside the well due to the pressure losses while in the CO_2-based case there's an important pressure increase inside the well. This is due to the fact that, in the horizontal section of the well, the CO_2 while heating up, decrease it's density resulting in a significant thermosyphon effect. The temperature increase and the overall output power is comparable between the two configurations.

Another interesting thing to notice is the effect of different geothermal gradients on the CO_2 behaviour. As shown in Figure 4, the outlet pressure decrease with time for lower gradients while the opposite happens for ∇T_{geo}=75°C/km.

This can be explained looking at Figure 5, which shows the profile of the fluid temperature and pressure inside the well.

For the ∇T_{geo}=75°C/km case, outlet pressure increase with time because the CO_2 will heat up less while descending into the vertical section of the well resulting in an denser fluid at horizontal section inlet and hence a stronger thermosyphon effect. On the other hand, for the ∇T_{geo}=50°C/km case, the effect of a denser CO_2 at the inlet of the horizontal section is mitigated by the greater reduction in outlet temperature which result in a denser ascending fluid.

https://doi.org/10.52202/077185-0109

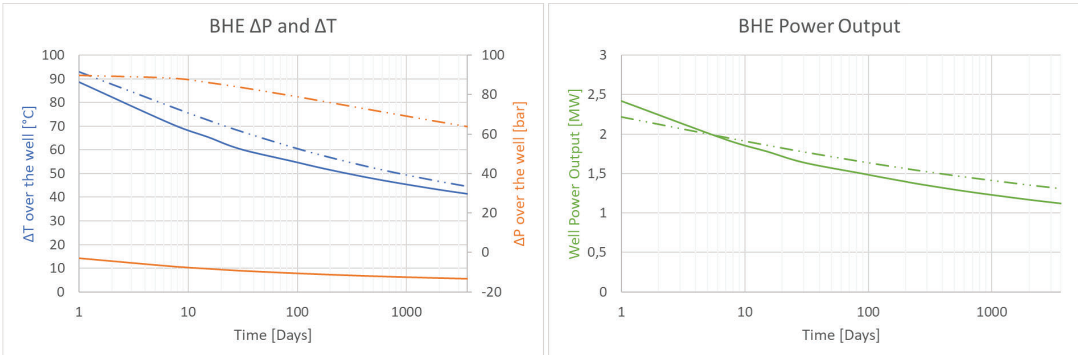

Figure 3: Comparison between water-based *(plain line)* and CO_2-based *(dash-dotted line)* well behaviour. *Left:* Temperature and Pressure increase inside the well with time. *Right:* Well power output with time. *(Conditions:* ∇T_{geo}*=50°C/km,* T_{sat}*=10°C,* $T_{water_{in}}$*=45°C)*

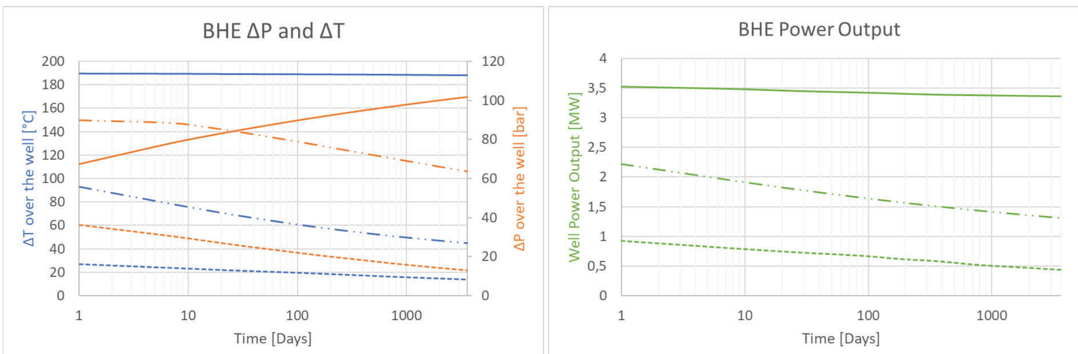

Figure 4: CO_2-based well behaviour for different geothermal gradient. *Left:* Temperature and Pressure increase inside the well. *Right:* Well power output with time. Plain line: ∇T_{geo}=75°C/km, Dash-dotted line: ∇T_{geo}=50°C/km, Dashed line: ∇T_{geo}=25°C/km *(Condition:* T_{sat}*=10°C)*

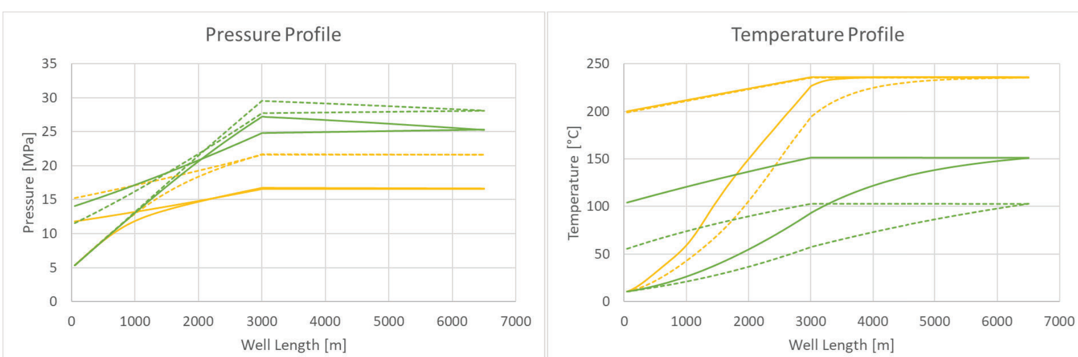

Figure 5: Pressure and Temperature profile inside the well for different geothermal gradient and times. *Plain line:* $t = 1year$ ∇T_{geo}*=75°C/km, dash-doted line* ∇T_{geo}*=50°C/km, dashed line* ∇T_{geo}*=25°C/km*

https://doi.org/10.52202/077185-0109

3.2 HTHP Behaviour

Regarding the HTHP, an example of its thermodynamic behaviour is depicted in Figure 6. The CO_2 is injected into the well as saturated liquid at a specific T_{sat} *(Point 1)*. It is then usually extracted from the well as a supercritical fluid, pressurised and heated up *(Point 2)*, mixed with the incoming re-compressed flash vapour from the separator *(points 3, 4 and 5)*, and compressed, if needed to reach the desired temperature level *(Point 6)*. The fluid is then cooled down to extract useful heat and then further cooled down to a specific temperature ($T_{turb_{in}}$) to decrease the vapour quality at the outlet of the expander.

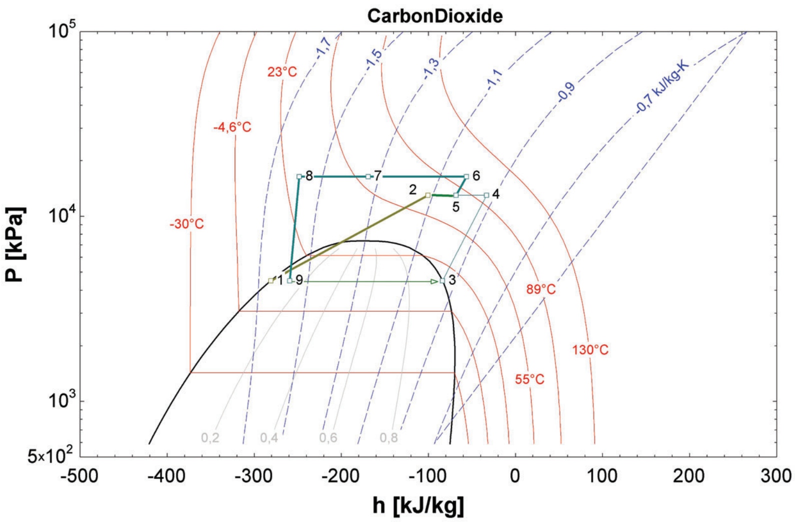

Figure 6: Depiction of the thermodynamic behaviour of the CO_2-based system from Figure 2 *(Considered condition: T_{max}=100°C, $T_{turb_{in}}$=30°C, $well_{depth}$=2km, $well_{lenght}$=6.5km, ∇T_{geo}=50°C/km, t=180days)*

As can be seen from Figure 8, the net power outlet, defined as in equation 10, usually increase with decreasing $T_{turb_{in}}$. This is because the specific work needed by the flash vapour re-compression ($\dot{w}_{comp2}$) is significantly higher to both the specific work of the turbine and of the HP compressor thus is imperative to avoid vapour generation in the expander as much as possible.

$$\dot{W}_{net} = \dot{W}_{turb} - \dot{W}_{comp1} - \dot{W}_{comp2} \tag{10}$$

Is interesting to notice that, in the condition depicted in Figure 8, with lower flow rates circulated into the well there could be the possibility to achieving some co-generation, highlighted by negative power requirements, even considering an higher supply temperature which is something that water based system can not do.

3.3 Economic Analysis

Finally, by comparing the LCOH results from water and CO_2-based systems, it appears clearly that water based systems are more suitable for being used for providing heat when higher geothermal gradients are present, while CO_2 can be an useful tool to provide sustainable heat even in regions with lower geothermal gradients.

The LCOH achieved with these kind of wells are usually high do to the high investment cost needed for well drilling (the considered well is expected to cost around 11M€). Despite this, the resulting LCOH are comparable with the ones obtained by other comparable technologies like pellet boilers (around 15c€/kWh) and solar thermal (around 10c€/kWh) (source: IEA, 2024)

https://doi.org/10.52202/077185-0109

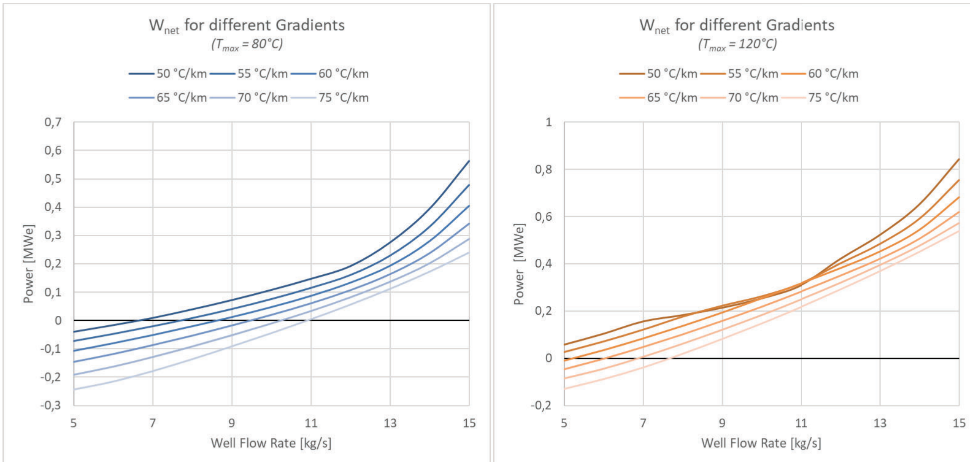

Figure 7: Effect of $\dot{m}_{well}$ on the CO_2-based system behaviour *(Considered condition: T_{max}=80°C, $well_{depth}$=3km, $well_{lenght}$=6.5km, t=10years)*

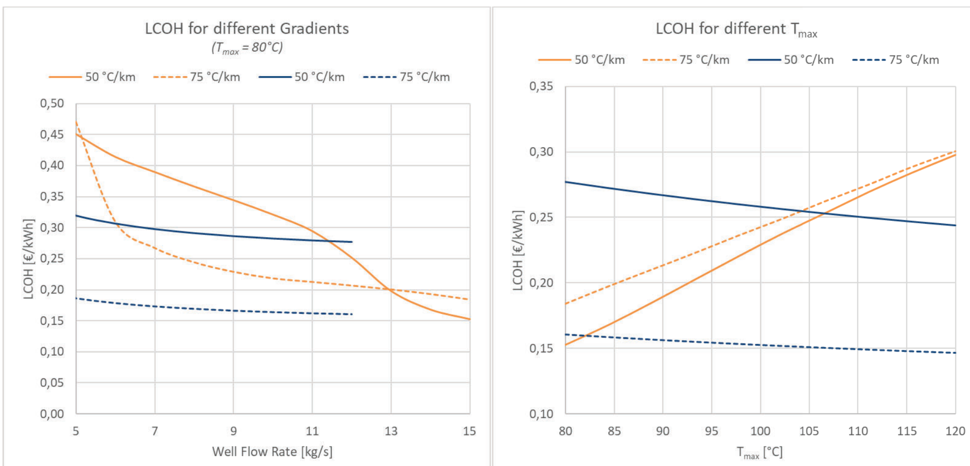

Figure 8: Comparison of the LCOH result for the water-based (blue lines) and CO_2-based (orange lines) systems *(Considered condition: $well_{depth}$=3km, $well_{lenght}$=6.5km, t=10years)*

4 Conclusion

The study demonstrates the viability and potential benefits of using CO_2 as a working fluid in geothermal-based high-temperature heat pumps (HTHPs).

The thermosyphon effect observed in the CO_2-based system results in a higher pressure increase within the well, leading to an efficient heat transfer process. This characteristic makes the CO_2-based system especially suitable for applications in areas with moderate geothermal resources and for limited required temperature, where conventional water-based systems might under-perform.

The economic analysis indicates that, although the initial investment costs for these kind of systems are substantial, the resulting LCOH is comparable to existing renewable heating technologies such as pellet boilers and solar thermal systems making these systems a viable option for the transition towards sustainable industrial heating solutions.

https://doi.org/10.52202/077185-0109

In summary, the use of CO2 as a working fluid in geothermal HTHPs presents a promising solution for providing reliable low-temperature heat, especially in regions with lower geothermal gradients. The study's findings highlight the potential of CO2-based systems to contribute to the decarbonization of the industrial heat sector, offering a sustainable and efficient alternative to conventional heating methods.

Acknowledgments

This research is part of the contribution of the University of Florence to the HOCLOOP project (Grant agreement ID: 101083558)

Nomenclature

Acronyms

BHE	Borehole Heat Exchanger
CHP	Combined Heat and Power
COP	Coefficient Of Performance
DH	District Heating
HE	Heat Exchanger
HTHP	High Temperature Heat Pump
LCOH	Levelized Cost Of Heat, *c€/kWh*

Economics

$C_{\square}$	Absolute cost, €
$c_{\square}$	Relative cost, *€/kW*
C_{om}	Operation and maintenance cost, *€/year*
C_{tot}	Overall investment cost of the system, €
h_y	Yearly operational time, *hours*
i	Interest rate
L_e	System operational life, *years*
OM_{ratio}	Ratio between C_{om} and C_{tot}

Geometrics

d_{well}	Well diameter, *m*
Δz_{well}	Depth of the horizontal section, *m*
A_{flow}	Flow area inside the well, m^2
L_{well}	Overall length of the well, *m*

Rocks Modelling

α_{rocks}	Rocks thermal diffusivity, m^2/s
γ	Euler's constant
ρ_{rocks}	Rocks thermal diffusivity, kg/m^3
k_{rocks}	Rocks thermal conductivity, $W/(m{\cdot}K)$
t_d	Non-dimensional Time
∇T_{geo}	Geothermal Gradient, $°C/m$
$c_{p_{rocks}}$	Rocks heat capacity, $J/(kg{\cdot}K)$

Thermodynamics

ΔT_{HE}	Temperature range in the main HE, $°C$
$\dot{m}_{well}$	Well Mass flow rate, *kg/s*
$\dot{Q}_{\square}$	Heat flux, *kW*
$\dot{W}_{\square}$	Mechanical power, *kW*
η_{comp}	Compressor isoentropic efficiency
η_{exergy}	Exergy efficiency
η_{turb}	Turbine isoentropic efficiency
$d\dot{q}_{tot}$	well heat flux over length, $kJ/(kg{\cdot}m)$
d_h	hydraulic diameter, *m*
dP_{loss}	well pressure losses over length, *Pa/m*
f	Darcy friction factor
T_{sat}	Saturation Temperature, $°C$

References

Adams, B. M. et al. (2021). "Estimating the Geothermal Electricity Generation Potential of Sedimentary Basins Using genGEO (the generalizable GEOthermal techno-economic simulator)". In: *ChemRxiv Preprint*.

Arpagaus, C. et al. (June 2018). "High temperature heat pumps: Market overview, state of the art, research status, refrigerants, and application potentials". In: *Energy* 152, pp. 985–1010. ISSN: 03605442. DOI: 10.1016/j.energy.2018.03.166.

https://doi.org/10.52202/077185-0109

Bilgen, E. and H. Takahashi (Jan. 2002). “Exergy analysis and experimental study of heat pump systems”. In: *Exergy, An International Journal* 2.4, pp. 259–265. ISSN: 11640235. DOI: 10.1016/S1164-0235(02)00083-3.

Churchill, S. W. (1977). “Friction-factor equatin spans over all fluid-flow regimes”. In: *Chemical Engineering* 84, pp. 91–92.

Dormand, J. and P. Prince (Mar. 1980). “A family of embedded Runge-Kutta formulae”. In: *Journal of Computational and Applied Mathematics* 6.1, pp. 19–26. ISSN: 03770427. DOI: 10.1016/0771-050X(80)90013-3.

European Project (2022). *A circular by design environmentally friendly geothermal energy solution based on a horizontal closed loop - HOCLOOP*.

Fiaschi, D. et al. (2022). “Development of an exergo-economic and exergo-environmental tool for power plant assessment: evaluation of a geothermal case study”. In: *34th International Conference on Efficiency, Cost, Optimization, Simulation and Environmental Impact of Energy Systems (ECOS 2021)*. Tokyo, Japan: ECOS 2021 Program Organizers, pp. 24–35. ISBN: 978-1-7138-4398-6. DOI: 10.52202/062738-0003. URL: http://www.proceedings.com/062738-0003.html.

Galoppi, G. et al. (Dec. 2015). “Feasibility Study of a Geothermal Power Plant with a Double-pipe Heat Exchanger”. In: *Energy Procedia* 81, pp. 193–204. ISSN: 18766102. DOI: 10.1016/j.egypro.2015.12.074.

Honore, A. (May 2019). *Decarbonization and industrial demand for gas in Europe*. Tech. rep. Oxford, United Kingdom: Oxford Institute for Energy Studies. DOI: 10.26889/9781784671396.

IEA (2022). *Heating*.

– (2024). *Levelized cost of heating (LCOH) for consumers, for selected space and water heating technologies and countries*. URL: https://www.iea.org/data-and-statistics/charts/levelized-cost-of-heating-lcoh-for-consumers-for-selected-space-and-water-heating-technologies-and-countries.

IEA-IETS (2014). *Application of Industrial Heat Pumps*. Tech. rep.

Klein, S. (June 2020). *EES – Engineering Equation Solver*.

Pieper, H. et al. (Aug. 2018). “Allocation of investment costs for large-scale heat pumps supplying district heating”. In: *Energy Procedia* 147, pp. 358–367. ISSN: 18766102. DOI: 10.1016/j.egypro.2018.07.104.

Sun, F. et al. (Sept. 2018a). “Geothermal energy extraction in CO2 rich basin using abandoned horizontal wells”. In: *Energy* 158, pp. 760–773. ISSN: 03605442. DOI: 10.1016/j.energy.2018.06.084.

– (Sept. 2018b). “Performance of geothermal energy extraction in a horizontal well by using CO2 as the working fluid”. In: *Energy Conversion and Management* 171, pp. 1529–1539. ISSN: 01968904. DOI: 10.1016/j.enconman.2018.06.092.

Ungar, P. (Mar. 2023). “Use of CO2 as working fluid in geothermal systems”. PhD thesis. Florence: University of Florence.

Ungar, P. et al. (2023). “Thermo-Economic Comparison of CO2 and Water as a Heat Carrier for Long-Distance Heat Transport from Geothermal Sources”. In: *36th International Conference on Efficiency, Cost, Optimization, Simulation and Environmental Impact of Energy Systems (ECOS 2023)*. Las Palmas De Gran Canaria, Spain: ECOS 2023, pp. 2593–2602. ISBN: 978-1-7138-7492-8. DOI: 10.52202/069564-0233.

Virtanen, P. et al. (Mar. 2020). “SciPy 1.0: fundamental algorithms for scientific computing in Python”. In: *Nature Methods* 17.3, pp. 261–272. ISSN: 1548-7091. DOI: 10.1038/s41592-019-0686-2.

Weiland, N. T., B. W. Lance, and S. R. Pidaparti (June 2019). “sCO2 Power Cycle Component Cost Correlations From DOE Data Spanning Multiple Scales and Applications”. In: *ASME Turbo Expo 2019: Turbomachinery Technical Conference and Exposition*. Phoenix, Arizona, USA: American Society of Mechanical Engineers. ISBN: 978-0-7918-5872-1. DOI: 10.1115/GT2019-90493.

Zhang, Y. et al. (2011). “A time-convolution approach for modeling heat exchange between a wellbore and surrounding formation”. In: *Geothermics* 40.4, pp. 261–266. ISSN: 03756505. DOI: 10.1016/j.geothermics.2011.08.003.

Zühlsdorf, B. et al. (Apr. 2019). “Analysis of technologies and potentials for heat pump-based process heat supply above 150°C”. In: *Energy Conversion and Management: X*. ISSN: 25901745. DOI: 10.1016/j.ecmx.2019.100011.

https://doi.org/10.52202/077185-0109

Appendix - Cost Correlation Table

Table 3: Cost correlation used in economic analysis

Comp.	**Cost Correlation**	**Notes**
Well	$C_{well} = a\left(0.105{L_{well}}^2 + 1776 L_{well}\Phi_{cas_{id}} + 2.735E5\right)$	*Result in [$], well diameter ($\Phi_{cas_{id}}$) and length ($L_{well}$) in [m], a = is a coefficient accounting for cost actualisation other uncertainties which is better detailed in the source (Source: Adams et al., 2021)*
Heat Exchangers	$C_{HE} = 49.45{UA_{HE}}^{0.7544}$	*Result in [$], Correlation for CO_2, UA_{HE} in [W/K], it is the product of the HE area and heat transfer coefficient (Source: Weiland et al., 2019)*
Compr.	$C_{comp} = 1230000\dot{W}_{comp}^{0.3992}$	*Result in [$], Correlation for CO_2, $\dot{W}_{comp}$ in [MW], is the compressor power (Source: Weiland et al., 2019)*
Turbine	$C_{turb} = 406200\dot{W}_{turb}^{0.8}$	*Result in [$], Correlation for CO_2, $\dot{W}_{turb}$ in [MW], is the turbine power (Source: Weiland et al., 2019)*
Heat Pump (Water)	$C_{HP} = 0.33667\dot{W}_{HP}$	*Result in [M€], $\dot{W}_{HP}$ in [MW], Correlation for $\dot{W}_{HP}$ up to 10MW, Only the heat pump acquisition cost has been considered. (Source: Pieper et al., 2018)*

https://doi.org/10.52202/077185-0109